Protein Engineering vol.15 no.3 pp.225–232, 2002

Impact of single-residue mutations on the structure and function of ovispirin/novispirin antimicrobial peptides

Monali V.Sawai[1], Alan J.Waring[2], William R.Kearney[3], Paul B.McCray, Jr[4], William R.Forsyth[5], Robert I.Lehrer[2,6] and Brian F.Tack[1]

[1]Department of Microbiology, [3]NMR Facility and [4]Department of Pediatrics, University of Iowa College of Medicine, Iowa City, IA 52242, [2]Department of Medicine, UCLA School of Medicine, Los Angeles, CA 90095 and [5]Department of Chemistry and Center for Biomolecular Structure and Function, Pennsylvania State University, University Park, PA 16802, USA

[6]To whom correspondence should be addressed. E-mail: rlehrer@mednet.ucla.edu

We studied three model antibacterial peptides that resembled the N-terminal 18 amino acids of SMAP-29, an α-helical, antimicrobial peptide of sheep. Although the parent compound, ovispirin-1 (KNLRR IIRKI IHIIK KYG), was potently antimicrobial, it was also highly cytotoxic to human epithelial cells and hemolytic for human erythrocytes. Single residue substitutions to ovispirin-1 yielded two substantially less cytotoxic peptides (novispirins), with intact antimicrobial properties. One of these, novispirin G-10, differed from ovispirin-1 only by containing glycine at position 10, instead of isoleucine. The other, novispirin T-7, contained threonine instead of isoleucine at position 7. We determined the three-dimensional solution structures of all three peptides by circular dichroism spectroscopy and two-dimensional nuclear magnetic resonance spectroscopy. Although all retained an amphipathic helical structure in 2,2,2-trifluoroethanol, they manifested subtle fine-structural changes that evidently impacted their activities greatly. These findings show that simple structural modifications can 'fine-tune' an antimicrobial peptide to minimize unwanted cytotoxicity while retaining its desired activity.

Keywords: amphipathic/antimicrobial peptides/NMR/solution structure

Introduction

There is considerable evidence that endogenous antimicrobial peptides play important roles in host defense against pathogenic microbes. For example, the blood neutrophils and other cells of mammals express a family of peptide precursors known as cathelicidins (Zanetti *et al.*, 1995, 2000; Gennaro *et al.*, 2000). The term cathelicidin derives from the highly conserved, N-terminal, 11 kDa 'cathelin' domain located proximal to the antimicrobial/LPS-binding domain. Cathelicidins are encoded by four-part genes (Gudmundsson *et al.*, 1995; Zhao *et al.*, 1995a,b). The fourth exon encodes the antimicrobial peptide, which may have an α-helical (Agerberth *et al.*, 1995), β-sheet (Zhao *et al.*, 1995a), proline-rich (Gudmundsson *et al.*, 1995; Zhao *et al.*, 1995b) or other structure.

These antimicrobial peptides are released when their cathelicidin precursor undergoes limited proteolysis by elastase (Scocchi *et al.*, 1992; Cole *et al.*, 2001) or by proteinase-3 (Sorensen *et al.*, 2001). Most of these peptides exert bactericidal activity by permeabilizing microbial membranes (Matsuzaki, 1998; Shai, 1999). However, some are also toxic and readily damage epithelial cells or cause hemolysis. Since many of the molecules that are abundant in bacterial membranes (e.g. lipopolysaccharide and phosphatidylglycerol) have a net negative charge, electrostatic interactions concentrate positively charged antimicrobial peptides on the membrane surface. Many cathelicidin peptides adopt an α-helical conformation in the presence of the organic co-solvent 2,2,2-trifluoroethanol (TFE) or when placed in other membrane-mimetic environments (Agerberth *et al.*, 1995; Chen *et al.*, 1995; Skerlavaj *et al.*, 1996; Gallo *et al.* 1997; Turner *et al.*, 1998; Travis *et al.*, 2000).

The present study deals with three model peptides that have some general resemblance to antimicrobial molecules found in nature. In its highly amphipathic structure and in the underlined portions of its primary sequence, ovispirin-1 (KNLRR IIRKI IHIIK KYG) resembles the N-terminal 18 amino acids of SMAP-29, (RGLRR LGRKI AHGVK KYG). The latter is a 29 residue, α-helical ovine cathelicidin peptide (Mahoney *et al.*, 1995; Skerlavaj *et al.*, 1999) with unusually potent antimicrobial activity (Travis, *et al.*, 2000). Both ovispirin-1 and SMAP-29 are hemolytic for human red blood cells and both cause substantial cytotoxicity features that could limit their use in humans. While attempting to determine if minor changes to the primary structure of ovispirin-1 might produce peptides with a more favorable ratio of therapeutic to toxic activity, we produced the two novispirin peptides described in this paper. Residue 10 of ovispirin-1 was changed from isoleucine to glycine (underlined) to produce novispirin G-10 (KNLRR IIRKG IHIIK KYG). Residue 7 of ovispirin-1 was changed from isoleucine to threonine (underlined) to make novispirin T-7 (KNLRR ITRKI IHIIK KYG).

This paper presents the three-dimensional solution structures of ovispirin-1 (PDB: 1HU5), novispirin G-10 (PDB: 1HU6) and novispirin T-7 (PDB: 1HU7) in the presence of TFE as determined by two-dimensional nuclear magnetic resonance (NMR) spectroscopy. We also describe the conformational analysis of these peptide antibiotics in the presence of TFE, lipopolysaccharide (LPS) and lipoteichoic acid (LTA) by circular dichroism (CD) spectroscopy. The effect of these changes on certain key antimicrobial, hemolytic and cytotoxic activities of these peptides is also described. Additional biological (Kalfa *et al.*, 2001; Saiman *et al.*, 2001) and structural (Yamaguchi, *et al.*, 2001) properties of ovispirin-1 were recently described elsewhere.

Materials and methods

Peptide synthesis and purification

Peptides were synthesized on an Applied Biosystems Model 433A synthesizer using solid-phase FastMoc chemistry and purified by reversed-phase high-performance liquid chromatography (RP-HPLC) on a Vydac 218TP1022 column. Separations were performed at a flow rate of 10 ml/min

employing a linear gradient (0 to 100% solvent B) of aqueous 0.1% trifluoroacetic acid (TFA) (solvent A) and acetonitrile containing 0.085% TFA (solvent B). Fractions were collected and monitored by analytical-scale RP-HPLC on a Vydac 218TP54 column employing isocratic elution conditions (40% solvent B) at a flow rate of 1 ml/min. Selected fractions were pooled and lyophilized for characterization by mass spectrometry and capillary electrophoresis. Mass measurements were performed on a Hewlett-Packard Model 1100 MSD equipped with an electrospray ionization source, using flow injection at 0.1 ml/min in 64% acetonitrile containing 0.05% TFA. Capillary electrophoresis was carried out on a Hewlett-Packard 3D instrument equipped with an 80.5 cm×75 μm i.d. fused-silica extended light-path capillary. Peptide concentrations were determined by quantitative amino acid analysis on a Beckman Model 6300 amino acid analyzer.

CD spectroscopy

CD analysis of ovispirin-1 and the two novispirins was performed on an AVIV 62DS spectropolarimeter (AVIV Associates, Lakewood, NJ) with thermoelectric temperature control. Spectra were recorded at 25°C in four solvent systems: 40 mM sodium phosphate buffer, pH 6.5 (buffer); buffer with 33% (v/v) trifluoroethanol (TFE) (Sigma); buffer with 1 mg/ml *Pseudomonas aeruginosa* lipopolysaccharide (Sigma); and buffer with 1 mg/ml *Staphylococcus aureus* lipoteichoic acid (Sigma). Peptide concentrations ranged from 84 to 100 μg/ml. Ellipticity scans were collected in triplicate, at 0.5 nm intervals, over the wavelength range 260–200 nm, with a light path of 0.1 cm in a Far-UV cell (Spectrocell, Oreland, PA). Final spectra representing the plots of mean residue ellipticity ([θ]) in deg cm^2 $dmol^{-1}$ vs wavelength (λ) in nm, were smoothed over an interval of five data points prior to plotting. The percentage helical content was estimated by the method of Chen (Chen *et al.*, 1974).

NMR sample preparation

The samples were dissolved in 0.8 ml of 50 mM Na_2HPO_4 buffer containing 40% TFE-D_3 (Cambridge Isotope Laboratories, Andover, MA) and 10% D_2O. They consisted of 1.6 mg of ovispirin-1 (0.88 mM), 1.8 mg of novispirin G-10 (1.02 mM) and 3.4 mg of novispirin T-7 (1.89 mM). The estimated pH values for these samples ranged from 6.16 to 6.38.

NMR experiments

NMR spectra were collected on a Varian Unity INOVA instrument at 500 MHz. Double quantum filtered correlation spectroscopy (DQF-COSY), total correlation spectroscopy (TOCSY) and nuclear Overhauser effect spectroscopy (NOESY) were performed at 25°C using standard procedures. The spectral width was 6 kHz in each dimension for all spectra. The H_2O signal was suppressed by presaturation during a 2.5 s relaxation delay in the NOESY and the TOCSY spectra and a 2 s relaxation delay in the DQF-COSY spectra. TOCSY and NOESY spectra were taken at 120 and 300 ms mixing times, respectively. In the NOESY and the TOCSY spectra the data sets were 1024 complex points in f_2 by 512 complex points in f_1 and 16 transients were averaged per f_1 increment. DQF-COSY spectra had a resolution of 2048 complex points in f_2 and 512 complex points in f_1 with an average of 32 transients per f_1 increment. The spectra were referenced to the TFE signal at 3.88 p.p.m. Baseline correction in f_2 was applied to the NOESY spectra prior to peak volume measurement. Spectral processing and NOESY peak volume measurement were done using the VNMR 6.1B software package.

Sequential resonance assignment

The resonance assignments for ovispirin-1 and the novispirins were obtained by employing the method of Wüthrich (Wüthrich, 1986). Proton spin systems of individual amino acid residues were identified from the DQF-COSY and the TOCSY spectra. The residues were then sequentially connected through the observed i, $i + 1$ NOE contacts. The chemical shifts for the proton spin system of Lys1 could not be detected for ovispirin-1, novispirin G-10 and novispirin T-7. Also missing was the chemical shift of the amide proton of Asn2.

Coupling constants

Coupling constants were measured from the DQF-COSY spectra and were corrected for line broadening. The number of $^3J_{HN\alpha}$ coupling constants measured for ovispirin-1, novispirin G-10 and novispirin T-7 was eight, thirteen and five, respectively. Two $^3J_{\alpha\beta}$ coupling constants were also measured for novispirin T-7.

Conformational restraints and structure calculation

Based on the NOESY peak volumes and the coupling constants, the necessary distance and dihedral angle constraints were generated for ovispirin-1, novispirin G-10 and novispirin T-7 using the Dynamics Algorithm for NMR Applications (DYANA) program (Güntert *et al.*, 1997). DYANA was also used to calculate and anneal structures consistent with these constraints. DYANA performs simulated annealing by molecular dynamics in torsion angle space (torsion angle dynamics). 172 distance constraints were used to calculate the ovispirin-1 structures. novispirin G-10 structures were based on 152 distance constraints, while novispirin T-7 structures were based on 163 distance constraints. Degenerate NOEs were excluded from structure calculation. For each peptide, 50 trial structures were generated with torsion angles chosen at random. NOE constraints were added to the standard force constant set using the DYANA target function multiplier of $\omega_0 = 10$ kJ/mol.Å^2. Torsion angle constraints were added using the default target function multiplier. Each structure was then annealed in 4000 steps from an initial temperature of 8000 K to 0 K, followed by 1000 further steps of conjugate gradient minimization. For each peptide, 20 structures with the lowest final target function value were subjected to conformational analysis and averaging using the Molecule Analysis and Molecule Display (MOLMOL) program (Koradi *et al.*, 1996).

Biological activity

Antimicrobial activity was tested by a previously described two-stage radial diffusion assay (Lehrer *et al.*, 1991; Turner *et al.*, 1998). Briefly, organisms were grown to mid-logarithmic phase and washed with 10 mM phosphate buffer, pH 7.4. Approximately 4×10^5 colony-forming units (CFU)/ml were incorporated into a thin (1.2 mm) underlay gel that contained 1% (w/v) agarose (Sigma A-6013), 0.3 mg/ml trypticase soy broth powder, 100 mM NaCl and 10 mM sodium phosphate buffer, pH 7.4. An array of 3.2 mm diameter wells allowed the introduction of 8 μl aliquots of the serially diluted peptide solutions, which were prepared in 0.01% acetic acid containing 0.1% human serum albumin to minimize adsorptive losses

After 3 h, a nutrient-rich overlay was poured and the plates were incubated overnight to allow surviving organisms to form microcolonies. Zone diameters were measured to the nearest 0.1 mm and expressed in units (1 unit = 0.1 mm), after

subtracting the diameter of the well. Because a linear relationship exists between the zone diameter and the $\log_{10}$ of the peptide concentration, the *x*-intercept of this line (determined by a least mean squares fit) was considered to represent the minimal effective concentration (MEC).

Hemolysis was measured conventionally by determining the release of hemoglobin after incubating a 2.5% (v/v) suspension of washed human erythrocytes in phosphate-buffered saline for 30 min at 37°C with the serially diluted peptides. The cells were then centrifuged and the optical density (OD) of the supernatant was measured at 540 nm. The '100% lysis' control was achieved by treating the red cells with 1% Triton X-100. The 'no lysis' control was prepared by incubating red cells in the absence of any peptide. The percentage hemolysis was calculated from the following equation:

$$\text{Hemolysis } (\%) = \frac{OD_{540}\text{ sample} - OD_{540}\text{ no lysis}}{OD_{540}\text{ 100\% lysis} - OD_{540}\text{ no lysis}} \times 100$$

Cytotoxicity was measured with a Cell Proliferation Kit I (Roche Diagnostics, Mannheim, Germany) that used MTT [3-(4,5-dimethylthiazol-2-yl)-2,5-diphenyltetrazolium] bromide as labeling reagent. These assays were performed in RPMI-1640 medium, supplemented with 10% fetal calf serum, 2 mM L-glutamine and 50 μg/ml gentamycin. Briefly, confluent target cells were detached with trypsin–EDTA, washed, resuspended in medium at 5×10^4 cells/ml and dispensed in 100 μl aliquots in 96 well Costar plates (Corning, Corning, NY). After incubation for 5 h at 37°C in room air with 5% CO_2 to allow the cells to adhere, peptide (various concentrations) was introduced and the incubation was continued for a further 20 h. Then, 10.0 μl of the MTT reagent were added to each well and the incubation was continued for an additional 4 h. Finally, 100.0 μl of extraction buffer were added to each well and, after overnight incubation at 37°C to extract the reduced formazan, the optical density was read in a SpectraMax 250 microplate spectrophotometer (Molecular Devices, Sunnyvale, CA) at 600 and 650 nm. The amount of reduced formazan (a measure of cellular metabolism) was proportional to $OD_{600} - OD_{650}$ and provided an index of cellular viability.

Results

Table I compares the hemolytic, cytotoxic and antimicrobial properties of ovispirin-1, novispirin G-10 and novispirin T-7. All three peptides had similar potency against Gram-negative bacteria (*P.aeruginosa*, *Stenotrophomonas maltophilia* and *Escherichia coli*) and ovispirin-1 and novispirin G-10 were equally effective against *Listeria monocytogenes*, a Gram-positive bacillus. Both novispirins were, however, somewhat less active than ovispirin-1 against *S.aureus*. Whereas novispirin G-10 caused minimal (2.5%) hemolysis of human erythrocytes when tested at 80 μg/ml, the same concentration of ovispirin-1 was profoundly hemolytic (70.2% lysis). novispirin T-7 caused 10% hemolysis when tested at the same concentration.

Ovispirin-1 was very cytotoxic for human epithelial cells, both the ME-180 (cervical) and A-549 (pulmonary) cell lines, with 50 μg/ml of ovispirin-1 reducing viability by 93.6% and 99.7%, respectively, as measured by a tetrazolium reduction assay. In contrast, 50 μg/ml of novispirin G-10 reduced the viability of ME-180 cells by 5.0% and of A549 cells by 14.6%. novispirin T-7 was more cytotoxic than novispirin G-10, but considerably less cytotoxic than ovispirin-1. Since novispirin G-10 differs from ovispirin-1 only by containing a glycine at position 10, instead of the isoleucine present in ovispirin-1, we performed structural studies in a search for explanations of their profound differences in function.

Figure 1 shows CD spectra of ovispirin-1, novispirin G-10 and novispirin T-7 in various solvent systems and Table II summarizes their percentage helical content. Unlike ovispirin-1, which showed weak helicity, the novispirin peptides existed as predominantly random coils in phosphate buffer. However, all three peptides assumed helical conformations when TFE, LPS or LTA was present. Under these conditions, ovispirin-1 was the most helical and novispirin G-10 was the least helical in each membrane-mimetic solvent system.

No intermolecular NOEs were evident and the one-dimensional spectra of the peptides in TFE displayed narrow linewidths, suggesting that peptide self-association was absent or minimal. Figure 2 summarizes the measured $^3J_{HN\alpha}$ coupling constants and the observed inter-residue NOE connectivities for the three peptides. The characteristic *i*, *i* + 3 and *i*, *i* + 4 NOEs are clearly indicative of helical conformations of these peptides in TFE. The helicity of these peptide antibiotics in TFE is further evident from their α-proton chemical shift indices (Wishart *et al.*, 1992), which are shown in Figure 3. The classification of the NMR distance and torsion angle constraints used in the structure calculation of the three peptides is given in Table III.

Figure 4 shows ribbon representations of ovispirin-1 and the two novispirins with the lowest final DYANA target function value. Figure 5 shows the backbone superpositions of the selected conformers of the three peptides. ovispirin-1 is a uniform α-helix over residues 4–16. novispirin G-10 shows an α-helix–hinge–3_{10} helix structural motif with residues 4–11 forming the α-helix, residues 12 and 13 forming the hinge and residues 14–16 forming the 3_{10} helix. novispirin T-7 is a well-defined α-helix over residues 7–17 with residues 3–6 forming a type IV turn.

The r.m.s.d. values over the residue range 2–18 for the selected 20 conformers of the three peptides are summarized in Table IV. The violation statistics for the selected conformers of each peptide are given in Table V.

Surface maps of the solution structures of ovispirin-1, novispirin G-10 and novispirin T-7 in TFE (Figure 6) clearly illustrate their amphipathic character. While the isoleucine residues contribute significantly to the hydrophobic faces in these structures, the positively charged residues are concentrated on the hydrophilic faces. These amphipathic helical peptide antibiotics exhibited hydrophobicity gradients along their backbones. When these gradients were calculated as described by Eisenberg (Eisenberg, 1984), they were 0.05 for ovispirin-1 and 0.05 and 0.06 for novispirin G-10 and T-7, respectively.

Discussion

In previous *in vitro* studies of mammalian cathelicidin peptides, ovine SMAP-29 and rabbit CAP-18 displayed potent broad-spectrum antibacterial activities that occurred rapidly and were retained in the presence of physiological NaCl concentrations (Travis *et al.*, 2000). Both peptides manifested a high net positive charge and both formed amphipathic helical structures with gradients of hydrophobicity along their helical backbones. When we made peptides containing 18–21 residues and corres-

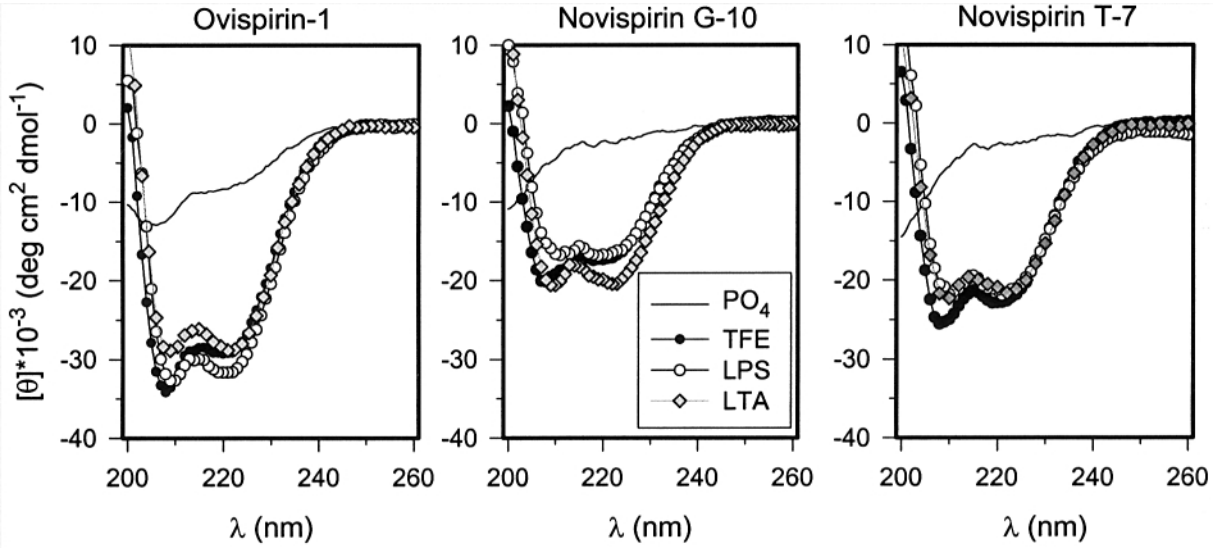

Fig. 1. CD spectra of ovispirin-1, novispirin G-10 and novispirin T-7 in various solvents. The plots show mean residue ellipticity ([θ]) in deg cm^2 $dmol^{-1}$ vs wavelength (λ) in nm.

Table I. Functional properties of ovispirin-1, novispirin G-10 and novispirin T-7

Target cells	Ovispirin-1	Novispirin G-10	Novispirin T-7
Hemolysis[a]	% Hemolysis at two peptide concentrations		
Human red blood cells	70.2% at 80 μg/ml 55.0% at 40 μg/ml	2.5% at 80 μg/ml 1.8% at 40 μg/ml	10.0% at 80 μg/ml 3.0% at 40 μg/ml
Cytotoxicity[b]	% Cytotoxicity at three peptide concentrations		
ME-180 cervical cells	100% at 200 μg/ml 93.6% at 50 μg/ml 55.3% at 25 μg/ml	33.2% at 200 μg/ml 5.0% at 50 μg/ml 7.1% at 25 μg/mll	81.5% at 200 μg/m 28.4% at 50 μg/ml 15.6% at 25 μg/ml
A-549 pulmonary cells	99.7% at 200 μg/ml 99.4% at 50 μg/ml 90.9% at 25 μg/ml	33.2% at 200 μg/ml 14.6% at 50 μg/ml 10.0% at 25 μg/ml	81.5% at 200 μg/ml 22.9% at 50 μg/ml 15.4% at 25 μg/ml
Antimicrobial activity[c]	Minimal effective concentration (μg/ml)		
P.aeruginosa, 9 strains	Range: 0.7–5.6 Mean: 1.66	Range: 0.11–12.7 Mean: 2.97	Range: 0.26–27.8 Mean: 4.64
S.maltophilia, 5 strains	Range: 0.5–2.2 Mean: 1.16	Range: 0.29–3.6 Mean: 1.18	Range: 0.32–1.75 Mean: 0.77
L.monocytogenes, EGD	1.5 ± 0.3 (n = 3)	1.4 ± 0.4 (n = 3)	2.4 ± 1.5 (n = 3)
S.aureus, 930918	1.0 ± 0.13 (n = 3)	4.6 ± 1.7 (n = 3)	3.3 ± 1.5 (n = 3)

[a]Hemolytic activity is expressed as % of maximum hemoglobin release after a 30 min incubation with peptide at the indicated concentration.
[b]Cytotoxicity was measured with an MTT kit (Boehringer-Mannheim) according to the manufacturer's instructions.
[b]Antimicrobial activity was measured by two stage radial diffusion assays, and the data show the minimal effective concentration (MEC) (mean ± S.E.M., n = 3).

Table II. % helical content values in various solvent systems for ovispirin-1, novispirin G-10 and novispirin T-7

Peptide	Phosphate	Phosphate + TFE	Phosphate + LPS	Phosphate + LTA
Ovispirin-1	23.6	86.1	93.3	85.0
Novispirin G-10	7.4	50.4	48.7	60.4
Novispirin T-7	8.0	66.8	64.1	63.9

Abbreviations: TFE, trifluoroethanol; LPS, lipopolysaccharide; LTA, lipoteichoic acid.

ponding to the N-terminus, C-terminus and mid-section of SMAP-29, the most active was SMAP $29_{[1–18]}$, an 18-mer (also called 'SMAP-29-18') that contained the N-terminal region of the parent molecule (Kalfa *et al.*, 2001; Saiman *et al.*, 2001). Although SMAP $29_{[1–18]}$ was not as active or salt tolerant as SMAP-29, it selectively permeabilized the outer membrane of *E.coli* (Wang,W., Hong,T., Wu,H., Orlov,D., Boo,L.M., Menzel,L., Guerrero,J., Waring,A.J. Tack.B.F. and Lehrer,R.I., unpublished work). The genesis of novispirins evolved from the foregoing studies.

Overall, ovispirin-1 (KNLRR IIRKI IHIIK KYG) and SMAP-$29_{[1–18]}$ (RGLRR LGRKI AHGVK KYG) are identical

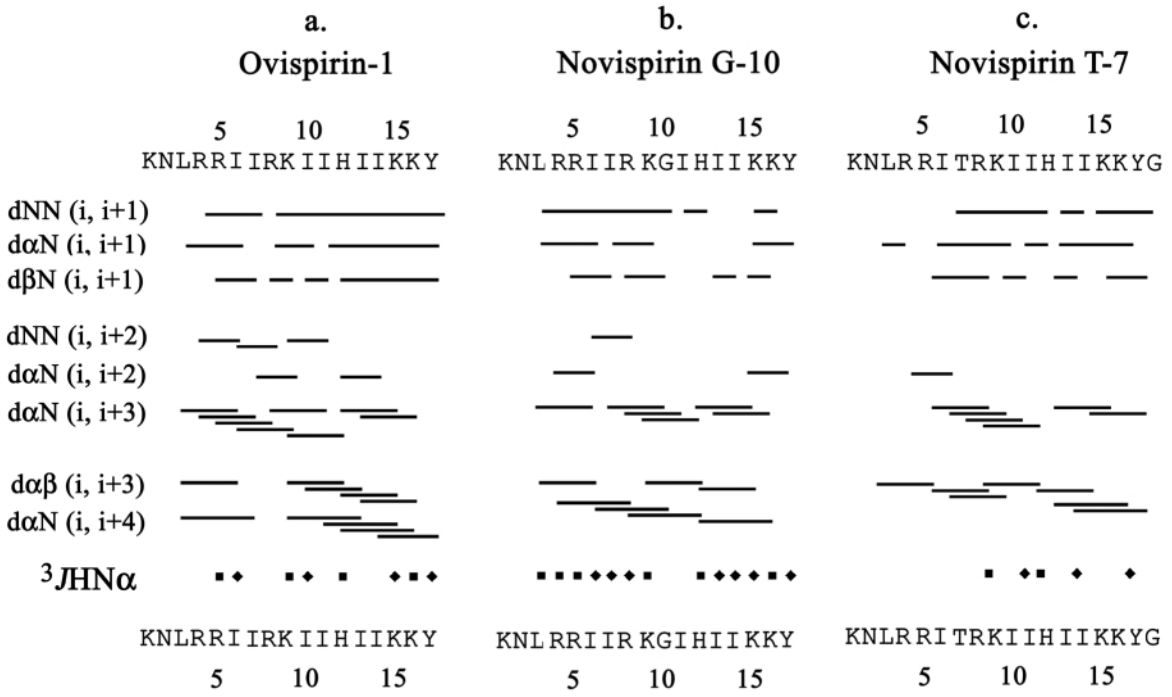

Fig. 2. Measured three-bond HN-α coupling constants and summary of observed inter-residue NOE connectivities for ovispirin-1, novispirin G-10 and novispirin T-7. $^{3}J_{HN\alpha}$ values <6 Hz are indicated by squares and those >6 Hz by diamonds.

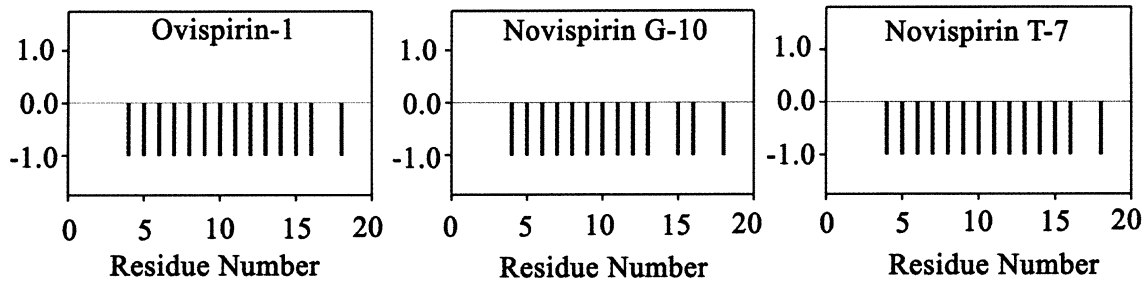

Fig. 3. The α-proton chemical shift indices for ovispirin-1, novispirin G-10 and novispirin T-7. Chemical shift index classifies α-protons based on whether their chemical shift is greater than (1), within (0) or less than (–1) the random coil value ± 0.1 p.p.m. According to the rules of chemical shift index, a group of three or more '1s' not interrupted by a '–1' indicates a β-strand and a group of four or more '–1s' not interrupted by a '1' indicates a helix. It should be noted that the chemical shift index for Lys1 could not be determined and that for Asn2 and Leu3 is 0 for all three peptides.

Table III. Classification of NMR distance and torsion angle constraints used in structure calculations for ovispirin-1, novispirin G-10 and novispirin T-7

Constraint type	Ovispirin-1	Novispirin G-10	Novispirin T-7
NOE distance constraints			
Intra-residue	90	90	89
Inter-residue	82	62	74
1 residue away	49	34	42
2 residues away	6	3	3
3 residues away	17	19	19
4 residues away	10	6	10
<2.50 Å	35	48	34
2.50–3.50 Å	82	52	71
>3.50 Å	55	52	58
Torsion angle constraints			
ϕ	8	13	5
χ_1	–	–	2

in 11/18 (61.1%) and 4/18 (22.2%) of the residues in ovispirin-1 contain the following conservative substitutions: R_1K, $A_{11}I$, L_6I and $V_{14}I$. In sharp contrast, the three glycine residues in SMAP-$29_{[1–18]}$ were replaced by very different residues in ovispirin-1 (G_2N, G_7I and $G_{13}I$). All of these changes were intended to create a peptide with enhanced helical stability and a more pronounced gradient of hydrophobicity along its backbone. Not only did ovispirin-1 show enhanced bactericidal activity and salt tolerance relative to SMAP-$29_{[1–18]}$ (Kalfa *et al.*, 2001; Saiman *et al.*, 2001), it also approximated the activity of the full-length SMAP-29 molecule in this regard.

In contrast to these favorable changes, ovispirin-1 also greatly exceeded SMAP-$29_{[1–18]}$ in its hemolytic and cytotoxic propensities for mammalian cells. Hoping to mitigate the cytotoxic properties of ovispirin-1 while preserving its bactericidal activity, we made four different molecules containing single residue substitutions, each intended to reduce the regional hydrophobicity of its apolar face (I_7T, I7G, $I_{10}T$, $I_{10}G$). We designated these molecules 'novispirins', further differentiating them by indicating the substitution that differentiated them from ovispirin-1. The most notable of these peptides was novispirin G-10 that had even greater anti-pseudomonal activity than ovispirin and about 10-fold less lytic activity.

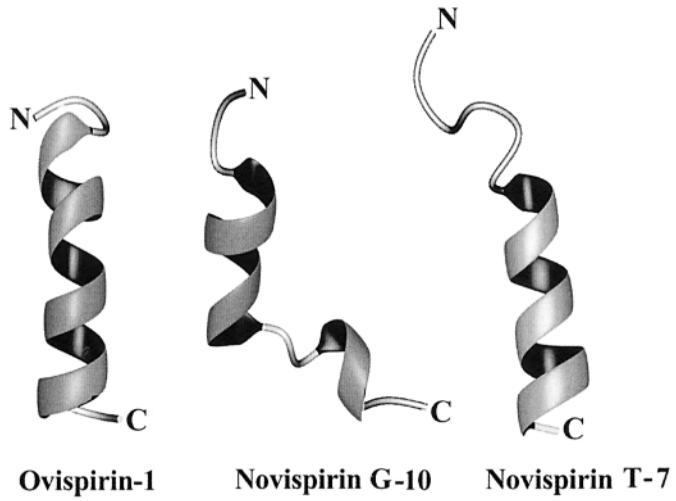

Fig. 4. Ribbon representations of ovispirin-1, novispirin G-10 and novispirin T-7conformers with the lowest DYANA target function value. This figure was made using MOLMOL.

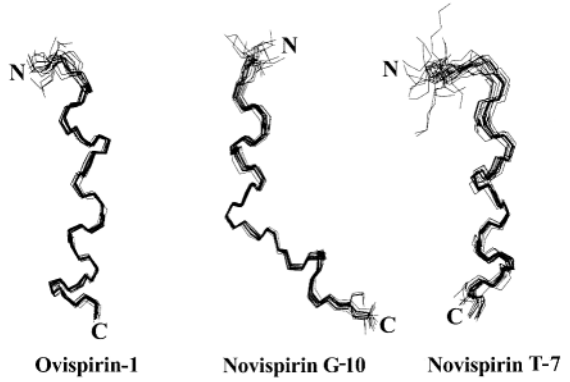

Fig. 5. Backbone superpositions of 20 selected conformers of ovispirin-1, novispirinG-10 and novispirin T-7. This figure was made using MOLMOL.

Table IV. Mean global r.m.s.d. values over the residue range 2–18 for the selected 20 conformers of ovispirin-1, novispirin G-10 and novispirin T-7

Peptide	Backbone r.m.s.d. (Å)	Heavy atom r.m.s.d. (Å)
Ovispirin-1	0.36 ± 0.12	1.30 ± 0.24
Novispirin G-10	0.57 ± 0.16	1.45 ± 0.26
Novispirin T-7	0.77 ± 0.26	1.83 ± 0.35

Table V. Violation statistics for the selected 20 conformers of ovispirin-1, novispirin G-10 and novispirin T-7

	Peptide	Mean r.m.s.d. from experimental restraints
NOE (Å)	Ovispirin-1	0.2041 ± 0.0006
	Novispirin G-10	0.274 ± 0.001
	Novispirin T-7	0.207 ± 0.001
Dihedrals (°)	Ovispirin-1	2.9 ± 0.7
	Novispirin G-10	4.0 ± 0.4
	Novispirin T-7	3.3 ± 0.0

In a recent 2D-NMR solution study, Gly7 formed a hinge between two helical segments of full length SMAP-29 and Gly18 resided in a highly flexible portion of the molecule. Consequently, restoring a glycine near the mid-portion of ovispirin-1 represents a partial return to the structure of native peptide, SMAP-29. It is interesting, in this light, that a glycine residue resides quite near the center of PGG (GLLRR LRKKI GEIFK KYG), the 'consensus' antimicrobial peptide designed by Tossi *et al.* (Tossi *et al.*, 1997).

Recent solid-state NMR studies of ovispirin-1 in lipid bilayer membranes were interpreted as indicating that the peptide forms a bent helix that undergoes rapid uniaxial rotation around the bilayer normal in the membrane–water interface (Yamaguchi *et al.*, 2001). In contrast to the straight helical structure manifested by the peptide in solution, when the peptide bound the lipid membrane the helix manifested a curvature spanning residues I_{14} to G_{18}.

Other workers have shown that relatively simple substitutions can greatly alter the ratio between antimicrobial and cytotoxic concentrations of antimicrobial peptides. For example, in studies with D-amino acid-containing analogues (diastereomers) of pardaxin and melittin (Oren and Shai, 1996, 1997), diastereomers that lost their α-helical structures became markedly less cytotoxic, even while retaining antibacterial activity. In these studies, the antimicrobial and cytotoxic peptides bound to and destabilized negatively charged phospholipid vesicles, but only the cytotoxic peptides bound to zwitterionic phospholipid vesicles. Unlike the non-cytotoxic peptides created in the above studies, introducing glycine-10 into ovispirin-1 altered but did not abolish the peptide's α-helical nature. Whereas ovispirin-1 formed a uniform α-helix over residues 4–16, the glycine modification in novispirin G-10 converted residues 12 and 13 into a hinge preceding a 3_{10} helix formed by residues 14–16. Presumably the markedly reduced cytolytic properties of novispirin G-10 reflect either the shortening of its rigid α-helical domain or its greater conformational flexibility or both. novispirin T-7, whose well-defined α-helix spanned residues 7–17, had cytotoxic properties intermediate between those of ovispirin-1 and novispirin G-10.

Lipopolysaccharide (LPS) and lipoteichoic acid (LTA) represent abundant polyanionic cell surface components characteristic of Gram-negative and Gram-positive bacteria, respectively. Several previous studies have demonstrated the ability of cathelicidin-derived α-helical antimicrobial peptides to bind LPS (Hirata *et al.*, 1994; Larrick *et al.*, 1994; Turner *et al.*, 1998), but LTA binding has been little studied. Our CD studies, which indicated that ovispirin-1 and the novispirins interacted with both LPS and LTA, are consistent with the notion that binding to both molecules is a common attribute of antimicrobial peptides (Scott *et al.*, 2000).

In the NMR structure of novispirin G-10, Gly10 itself is in the α-helical section of the peptide. However, Gly10 substitution results in a hinge involving His12 and Ile13 (observed in all 20 selected conformers). According to the chemical shift index, the random coil α proton chemical shift values for histidine and isoleucine are 4.63 ± 0.10 and 3.95 ± 0.10, respectively. In ovispirin-1, the α-proton chemical shift values for His12, Ile13 and Ile14 were 4.19, 3.73 and 3.69, respectively. The corresponding values in novispirin T-7 were 4.19, 3.74 and 3.69. In novispirin G-10 however, the corresponding values were 4.31, 3.84 and 3.85. Thus in novispirin G-10, the α-proton chemical shift values for His12, Ile13 and Ile14 are much closer to the random coil values than in ovispirin-1 or novispirin T-7. In fact, Ile13 in novispirin G-10 missed a chemical shift index of 0 only by 0.01, while Ile14 showed a chemical shift index of 0. Similar to ovispirin-1 and novispirin

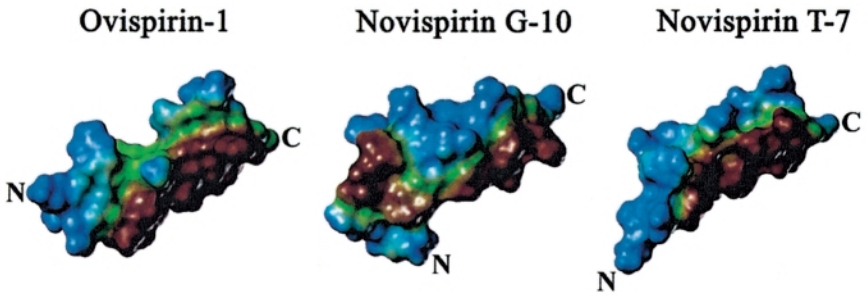

Fig. 6. Surface maps of ovispirin-1, novispirin G-10 and novispirin T-7 conformers with the lowest DYANA target function value. This figure was made using SYBYL 6.5 (Tripos, St. Louis, MO). Lipophobic areas are blue and lipophilic areas are reddish brown.

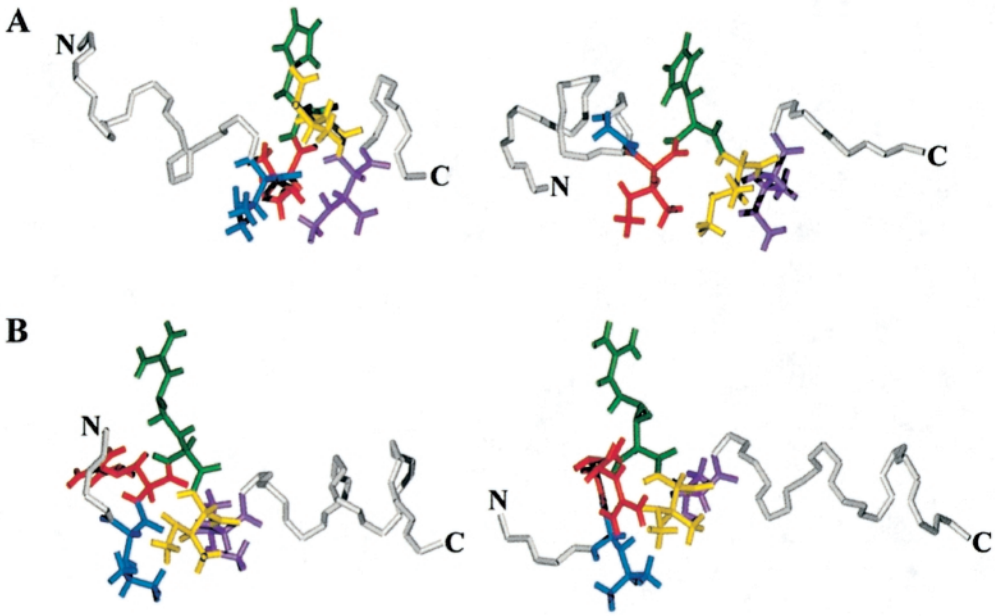

Fig. 7. Comparison of the solution structures of ovispirin-1 and novispirin G-10 over residues 10–14 (**A**) and that of the solution structures of ovispirin-1 and novispirin T-7 over residues 3–7 (**B**). Residues 3 and 10 are blue, residues 4 and 11 are red, residues 5 and 12 are dark green, residues 6 and 13 are gold and residues 7 and 14 are dark violet. This figure was made using MOLMOL.

T-7, NOEs indicative of helical structure were observed over residues His12–Lys16 in novispirin G-10. However, the intensities of these NOEs differed. For example, the peak volumes (normalized to the NOE between Tyr17 β-protons) of the Ile13 α-Lys_{16} amide NOE were 0.058 and 0.067 in ovispirin-1 and novispirin T-7, respectively. In novispirin G-10, however, the corresponding peak volume was 0.244.

The solution structures of ovispirin-1 and novispirin G-10 over residues 10–14 are compared in Figure 7A. In ovispirin-1, the side chains of Ile10, Ile11 and Ile14 are situated on the hydrophobic face of the molecule while the His12 side chain is located on the hydrophilic face. The Ile13 side chain is located near the hydrophobic–hydrophilic interface of the molecule more or less parallel to the His12 side chain. Indeed, a clear NOE contact was observed between the δ-proton of His_{12} and the γCH_3 group of Ile13. The isolation of the side chain of Ile13 from those of Ile10, Ile11 and Ile14 is most likely attributable to steric hindrance. In novispirin G-10 however, the presence of Gly10 allows the side chain of Ile13 to orient on the hydrophobic face joining the side chains of Ile11 and Ile14 with His12 once again located on the hydrophilic face. It appears that the substitution of Ile10 by a glycine residue creates a void in the hydrophobic face of the molecule that the side chain of Ile13 fills. Whether these structural differences have any impact on cytotoxic and hemolytic events is uncertain.

The α-helical component of the novispirin T-7 solution structure includes Thr7. There exists a possibility that the type IV turn involving Leu3–Ile6 observed in 19 of the 20 selected conformers in novispirin T-7 could be helical since the chemical shift indices for ovispirin-1 and novispirin T-7 are identical. Similarly to ovispirin-1 and novispirin G-10, an *i*, *i* + 3 NOE indicative of helical conformation was observed between Leu3 α-proton and Ile6 β-proton in novispirin T-7. However, while the peak volumes (normalized to the NOE between Tyr17 β-protons) of this NOE were 0.125 and 0.126 in ovispirin-1 and novispirin G-10, respectively, the corresponding peak volume was 0.032 in novispirin T-7. The random coil α-proton chemical shift value for arginine is 4.38 ± 0.10 according to the chemical shift index. The Arg4 α-proton chemical shift of 4.03 in novispirin T-7 was much closer to the random coil value that that of 3.88 in ovispirin-1 and 3.93 in novispirin G-10. In novispirin T-7, *i*, *i* + 2 NOE connectivities were observed between Arg5 and Thr7 (Arg5 α-Thr7 amide, Arg5 α-Thr7 β and Arg5 α-Thr7 γCH_3). Analogous contacts were missing in ovispirin-1 and novispirin G-10. Figure 7B compares the solution structures of ovispirin-1 and novispirin T-7 over

residues 3–7. The polarity but not the positioning of the Thr7 side chain in the three-dimensional solution structure of novispirin T-7 is very different from that of the Ile7 side chain in ovispirin-1. The orientation of the Arg4 side chain is different in ovispirin-1 and novispirin T-7.

The highly amphipathic arrangements of ovispirin-1, novispirin G-10 and novispirin T-7 are consistent with a mechanism for bacterial membrane destruction that involves burial of their hydrophobic faces within the lipid bilayer, aided by the interaction of their charged hydrophilic faces with the polar phospholipid head groups. The NMR solution structure of the rabbit cathelicidin-derived peptide $CAP18_{[106–137]}$ has been determined (Chen *et al.*, 1995). This peptide was found to be in a rigid, end to end α-helical conformation in the presence of 30% TFE with the cationic and hydrophobic groups separated into patches and stripes.

In summary, while ovispirin-1 and novispirin G-10 both had solution structures that were helical and amphipathic in the presence of TFE, a relatively simple change in their primary structure (a single glycine–isoleucine exchange) had profound effects on their respective toxicities for human erythrocytes and epithelial cells. Although long, rigid and highly amphipathic peptide domains may be capable of injuring host cells, simple structural modifications can ‘fine tune’ these to increase their potential utility.

Acknowledgements

This work was supported, in part, by grants from the National Institutes of Health: AI-43934 and AI-37945 (to R.I.L.), NIH P50 HL-61234 (to B.F.T. and P.B.M.), the Cystic Fibrosis Foundation (to B.F.T. and P.B.M., 97ZO) and the University of Iowa College of Medicine (to W.R.K.).

References

Agerberth,B., Gunne,H., Odeberg,J., Kogner,P., Boman,H.G. and Gudmundsson,G.H. (1995) *Proc. Natl Acad. Sci. USA*, **92**, 195–199.

Chen,C., Brock,R., Luh,F., Chou,P.J., Larrick,J.W., Huang,R.F. and Huang,T.H. (1995) *FEBS Lett.*, **370**, 46–52.

Chen,Y.H., Yang,J.T. and Chau,K.H. (1974) *Biochemistry*, **13**, 3350–3359.

Cole,A.M., Shi,J., Ceccarelli,A., Kim,Y.H., Park,A. and Ganz,T. (2001) *Blood*, **97**, 297–304.

Eisenberg,D. (1984) *Annu. Rev. Biochem.*, **53**, 595–623.

Gallo,R.L., Kim,K.J., Bernfield,M., Kozak,C.A., Zanetti,M., Merluzzi,L. and Gennaro,R. (1997) *J. Biol. Chem.*, **272**, 13088–13093.

Gennaro,R. and Zanetti,M. (2000) *Biopolymers*, **55**, 31–49.

Gudmundsson,G.H., Magnusson,K.P., Chowdhary,B.P., Johansson,M., Andersson,L. and Boman,H.G. (1995) *Proc. Natl Acad. Sci. USA*, **92**, 7085–7089.

Güntert,P., Mumenthaler,C. and Wüthrich,K. (1997) *J. Mol. Biol.*, **273**, 283–298.

Hirata,M., Shimomura,Y., Yoshida,M., Morgan,J.G., Palings,I., Wilson,D., Yen,M.H., Wright,S.C. and Larrick,J.W. (1994) *Infect. Immun.*, **62**, 1421–1426.

Kalfa,V.C., Jia,H.V.P., Kunkle,R.A., McCray,P.B.,Jr, Tack,B.F. and Brogden,K.A. (2001) *Antimicrob. Agents Chemother.*, **45**, 3256–3261.

Koradi,R., Billeter,M. and Wüthrich,K. (1996) *J. Mol. Graphics*, **14**, 51–55.

Larrick,J.W., Hirata,M., Zheng,H., Zhong,J., Bolin,D., Cavaillon,J.M., Warren,H.S. and Wright,S.C. (1994) *J. Immunol.*, **152**, 231–240.

Lehrer,R.I., Rosenman, M., Harwig, S. S. L., Jackson, R. and Eisenhauer, P. (1991) *J. Immunol. Methods*, **137**, 167–173.

Mahoney,M.M., Lee,A.Y., Brezinski-Caliguri,D.J. and Huttner,K.M. (1995) *FEBS Lett.*, **377**, 519–522.

Matsuzaki,K. (1998) *Biochim. Biophys. Acta*, **1376**, 391–400.

Oren,Z. and Shai,Y. (1996) *Eur. J. Biochem.*, **237**, 303–310.

Oren,Z. and Shai,Y. (1997) *Biochemistry*, **36**, 1826–1835.

Saiman,L., Tabibi,S., Starner,T.D., Gabriel,P.S., Winokur,P.L., Jia,H.P., McCray,P.B.,Jr and Tack,B.F. (2001) *Antimicrob. Agents Chemother.*, **45**, 2838–2844.

Scocchi,M., Skerlavaj,B., Romeo,D. and Gennaro,R. (1992) *Eur. J. Biochem.*, **209**, 589–595.

Scott,M.G., Vreugdenhil,A.C., Buurman,W.A., Hancock,R.E. and Gold,M.R. (2000) *J. Immunol.*, **164**, 549–553.

Shai,Y. (1999) *Biochim. Biophys. Acta*, **1462**, 55–70.

Skerlavaj,B., Gennaro,R., Bagella,L., Merluzzi,L., Risso,A. and Zanetti,M. (1996) *J. Biol. Chem.*, **271**, 28375–28381.

Skerlavaj,B., Benincasa,M., Risso,A., Zanetti,M. and Gennaro,R. (1999) *FEBS Lett.*, **463**, 58–62.

Sorensen,O.E., Follin,P., Johnsen,A.H., Calafat,J., Tjabringa,G.S., Hiemstra,P.S. and Borregaard,N. (2001) *Blood*, **97**, 3951–3959.

Tossi,A., Tarantino,C. and Romeo,D. (1997) *Eur. J. Biochem.*, **250**, 549–558.

Travis,S.M., Anderson,N.N., Forsyth,W.R., Espiritu,C., Conway,B.D., Greenberg,E.P., McCray,P.B.,Jr, Lehrer,R.I., Welsh,M.J. and Tack,B.F.(2000) *Infect. Immun.*, **68**, 2748–2755.

Turner,J., Cho,Y., Dinh,N.N., Waring,A.J. and Lehrer,R.I. (1998) *Antimicrob. Agents Chemother.*, **42**, 2206–2214.

Yamaguchi,S., Huster,D., Waring,A., Lehrer,R.I., Kearney,W., Tack,B.F. and Hong,M. (2001) *Biophys. J.*, **81**, 2203–2214.

Wishart,D.S., Sykes,B.D. and Richards,F.M. (1992) *Biochemistry*, **31**, 1647–1651.

Wüthrich,K. (1986) *NMR of Proteins and Nucleic Acids.* Wiley, New York.

Zanetti,M., Gennaro,R. and Romeo,D. (1995) *FEBS Lett.*, **374**, 1–5.

Zanetti,M., Gennaro,R., Scocchi,M. and Skerlavaj,B. (2000) *Adv. Exp. Med. Biol.*, **479**, 203–218.

Zhao,C., Ganz,T. and Lehrer,R.I. (1995a) *FEBS Lett.*, **368**, 197–202.

Zhao,C., Ganz,T. and Lehrer,R.I. (1995b) *FEBS Lett.*, **376**, 130–134.

Received August 6, 2001; revised October 23, 2001; accepted December 20, 2001